



Mechanical Modification of Nanomaterials on Fully Saturated Concrete in Groundwater Reservoir Under Long-Term Water Immersion

XianJie Hao^{1,2,3*}, Yingnan Wei⁴, Zeyu Chen³, Honglan Zhang³, Yifan Niu³, Kai Chen³ and Ruilai Huang³

¹Beijing Key Laboratory for Precise Mining of Intergrown Energy and Resources, China University of Mining and Technology (Beijing), Beijing, China, ²State Key laboratory of Coal Resources and Safe Mining, China University of Mining and Technology (Beijing), Beijing, China, ³School of Energy and Mining Engineering, China University of Mining and Technology (Beijing), Beijing, China, ⁴Zhengzhou Coal Mining Machinery (Group) Co., Ltd, Zhengzhou, China

OPEN ACCESS

Edited by:

Lijie Guo,
Beijing General Research Institute of
Mining and Metallurgy, China

Reviewed by:

Erol Yilmaz,
Recep Tayyip Erdoğan University,
Turkey
Shiqi Dong,
University of California, Los Angeles,
United States

*Correspondence:

XianJie Hao
haoxianjie@cumtb.edu.cn

Specialty section:

This article was submitted to
Structural Materials,
a section of the journal
Frontiers in Materials

Received: 29 April 2021

Accepted: 22 June 2021

Published: 15 July 2021

Citation:

Hao X, Wei Y, Chen Z, Zhang H, Niu Y,
Chen K and Huang R (2021)
Mechanical Modification of
Nanomaterials on Fully Saturated
Concrete in Groundwater Reservoir
Under Long-Term Water Immersion.
Front. Mater. 8:702308.
doi: 10.3389/fmats.2021.702308

With the increasing number of hydraulic structures in service, many scholars have investigated the performance of saturated concrete, however, there are few studies on the influences of different contents and types of nanomaterials on the performance of fully saturated concrete. In this paper, a series of experiments on concrete with different contents of nano SiO₂, nano Al₂O₃ and nano TiO₂ are performed, such as electron mirror scanning, uniaxial compression, acoustic emission, etc., and the microstructure, mechanical properties of samples are compared and analyzed. The results show that: 1) By the addition of various kinds of nanomaterials to saturated concrete, the microstructure of saturated concrete is significantly improved, and the compactness and integrity of the slurry are improved 2) The mechanical properties of saturated concrete are significantly improved by the addition of 3 wt% nanomaterials. And the compressive strength of the saturated concrete sample containing 3 wt% nano-Al₂O₃ is the largest and the deformation modulus of the saturated concrete sample containing 6 wt% nano-Al₂O₃ is the largest. 3) Compared with dry concrete, when the concrete is saturated, the modifying effect of nanomaterials on the mechanical properties of concrete is weakened. The results of this study have important guiding significance for the study of the nano-modification and the safe operation of hydraulic structures.

Keywords: saturated concrete, nanomaterials, microstructure, mechanical properties, modification

INTRODUCTION

Concrete is widely used in various construction projects because of its low cost and abundance of constituent materials (Zuo et al., 2018; Lu et al., 2019). It is most commonly used in building structures, therefore, the safety of concrete structures is very important. The mechanical properties of concrete are the foundation for ensuring the safety and stability of concrete structures.

Due to the presence of many pores and other defects in concrete, it is easily damaged: to improve the mechanical properties of concrete materials, admixtures are often used (Cao et al., 2020; Cao et al., 2021). Nanomaterials have a small particle size and high (and stable) specific surface energy. Therefore, nanomaterials are often used as admixtures to improve the mechanical properties of concrete. Much work so far has focused on nano-SiO₂, nano-Al₂O₃ and nano-TiO₂ due to their

dominate advantages in compressive strength, microstructure and price. Said et al. (Said et al., 2012) observed the significant improvement in concrete incorporating nano-silica in terms of reactivity, strength development, refinement of pore structure, and densification of the interfacial transition zone. Jalal et al. (Jalal et al., 2015) indicated the mechanical and transport properties improved in concrete containing nanomaterials especially when using a blend of silica nanoparticles and silica fume. Zhou et al. (Zhou et al., 2019) studied the hydration of Portland cement blended with 5% of nano-alumina, and identified a chemical effect of nano-alumina alongside the well-known filler effect, which is related to its solubility in pore fluids. Shaikh et al. (Shaikh et al., 2017) studied the effect of mixing methods of nano-silica on properties of recycled aggregate concrete. Du et al. (Du et al., 2015) investigated the influence of nano-silica on the mechanical and transport properties of lightweight concrete. Liu et al. (Liu et al., 2018) concluded that the effects of nano-SiO₂ on promoting the hydration, refining the pore structure, narrowing the width of microcrack, and thus reducing the permeability of cement paste become much clearer as the W/C ratio decreases. Yang et al. (Yang et al., 2019) indicated that nano-Al₂O₃ can be used for improving the chloride binding capacity of cement. Li et al. (Li et al., 2006a) showed that the addition of nano-Al₂O₃ to concrete increases the compactness of the interfacial transition zone, decreases the porosity of the cement, and increases the elastic modulus and compressive strength of the concrete. Deng et al. (Deng, 2012) demonstrated that nano-TiO₂, as a partial substitute for cement, can improve the compressive performance of concrete to some extent. Zhang et al. (Zhang et al., 2015) showed that nano-TiO₂ increases the compressive strength of cement mortar through its acceleration of cement hydration and the pore-refining effect. Hong et al. (Hong et al., 2020) proved that nano-clay could promote the hydration process of cement grouting material, and thus it weakens the chloride ion erosion due to the porosity reduction effect. It can be seen from the literature that nanomaterials can not only fill the pores in concrete, but also participate in and promote the hydration reaction of concrete materials. Adding nanomaterials to the concrete can improve the microstructure of the concrete and can increase its compressive strength and elastic modulus.

Some concrete structures must survive in water for a long time (e.g., dams and artificial dams in groundwater reservoirs). The mechanical properties of the concrete will be affected by water. Due to the surrounding water pressure and initial defects such as internal pores and cracks, the internal pores and cracks of concrete structures are filled with water, saturating the concrete. Many scholars have studied the differences in mechanical performance between saturated and dry concrete. Research shows that the strength of saturated concrete is lower than that of dry concrete, while the static and dynamic modulus is higher (Rossi et al., 1992; Ross et al., 1996; Yaman et al., 2002a; Yaman et al., 2002b; Wang and Li, 2007). Zheng et al. (Zheng and Li, 2010) proposed a method of predicting the elastic modulus of dry and saturated concrete based on the micromechanics of composite materials. Jin et al. (Jin et al., 2012) studied the effect of pore-water on the mechanical properties of saturated

concrete and established relationships between the water content and the elastic parameters of saturated concrete. Kaji et al. (Kaji and Fujiyama, 2014) found that the compressive strength of saturated concrete increases with the strain rate. Wang et al. (Wang et al., 2016) investigated the effect of saturation on the behavior of concrete under biaxial compression: the results indicated that the static compressive strength of saturated concrete is lower than that of dry concrete, but the dynamic strength of saturated concrete is higher than that of dry concrete. Siddiqui et al. (Siddiqui et al., 2016) developed an approximate analytical model for the axial strain and internal water pressure development in a saturated concrete cylinder. Bian et al. (Bian et al., 2017) proposed a coupled elastoplastic damage model to describe the mechanical behavior of saturated and dry concrete over a wide range of confining pressures. It can be seen from the published literature that the mechanical properties of concrete are significantly affected by saturation. The static strength of saturated concrete is reduced compared with dry concrete, but the dynamic strength and modulus are increased compared with dry concrete.

Due to the low static strength of saturated concrete, it is unsatisfactory in some engineering applications. For example, artificial dams of groundwater reservoir will always be subject to seepage in service, and the artificial dam often requires rebuilding.

The mechanical properties of saturated concrete may be improved by addition of nanomaterials. Adding nanomaterials may be a better measure for saturated concrete. Although many scholars have done a lot of research on saturated concrete, especially the difference between saturated concrete and dry concrete, few have studied the modifying effect of nanomaterials on saturated concrete, especially the difference in the effect of different nanomaterials. With the increasing number of construction projects in water, to ensure the safety stability and service life of these hydraulic structures, it is becoming more important to study the modifying effect of nanomaterials on the mechanical properties of saturated concrete.

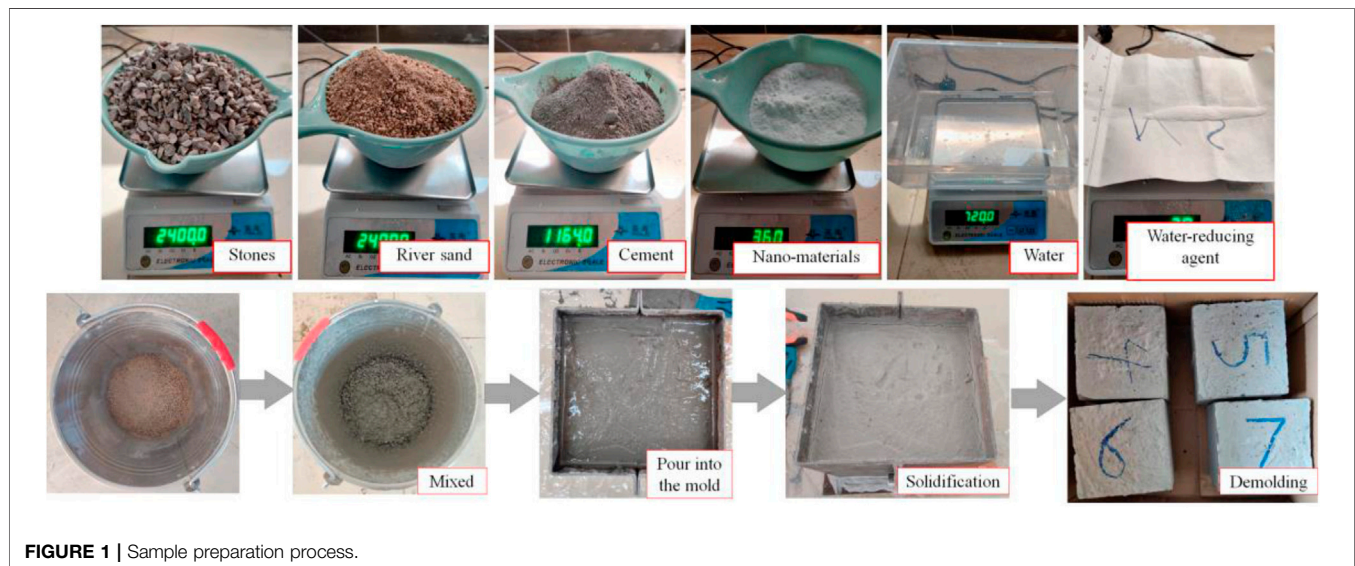
The research object of this paper is fully saturated concrete, the purpose is to study the influence of different types and contents of nanomaterials on the mechanical properties of saturated concrete, and to compare the modifying effects of different types and contents of nanomaterials in this paper. A series of experiments on saturated concrete specimens with different types and contents of nanomaterials are conducted. In *Sample Preparation*, three nanomaterials (nano-SiO₂, nano-Al₂O₃, and nano-TiO₂) are selected as admixtures to prepare different types of nano-saturated concrete samples. In *Composition and Microstructure*, the composition and microstructure of the nano-saturated concrete samples are tested by XRF and SEM. In *Results and Analysis*, wave velocity tests and uniaxial compression tests are performed on saturated concrete samples, and the test results presented therein. In *Discussion*, the mechanical parameters such as strength, modulus of different nano-saturated concrete samples are compared. In *Conclusion*, the saturated concrete containing nanomaterials is compared with dry concrete containing the same nanomaterials (data sourced from the literature), and the different modifying

TABLE 1 | Chemical composition of Portland cement (PO42.5).

Chemical composition	CaO	SiO ₂	Al ₂ O ₃	TiO ₂	MgO	SO ₃	K ₂ O
Content (%)	59.72	21.15	5.93	0.51	2.31	2.23	0.53

TABLE 2 | Concrete mixes.

Type	Cement/g	River sand/g	Stones/g	Water/g	Water-reducing agent/g	Nano-SiO ₂ /g	Nano-Al ₂ O ₃ /g	Nano-TiO ₂ /g
Ordinary concrete	1,200	2,400	2,400	720	3			
3 wt% Nano-SiO ₂ sample	1,164	2,400	2,400	720	3	36		
6 wt% Nano-SiO ₂ sample	1,128	2,400	2,400	720	3	72		
3 wt% Nano-Al ₂ O ₃ sample	1,164	2,400	2,400	720	3		36	
6 wt% Nano-Al ₂ O ₃ sample	1,128	2,400	2,400	720	3		72	
3 wt% Nano-TiO ₂ sample	1,164	2,400	2,400	720	3			36
6 wt% Nano-TiO ₂ sample	1,128	2,400	2,400	720	3			72

**FIGURE 1** | Sample preparation process.

effects of nanomaterials on the mechanical properties of saturated concrete and dry concrete are analyzed. The results of this study have important guiding significance for the study of the nano-modification of saturated concrete mechanical properties and the safe operation of construction engineering work in water.

SAMPLE PREPARATION

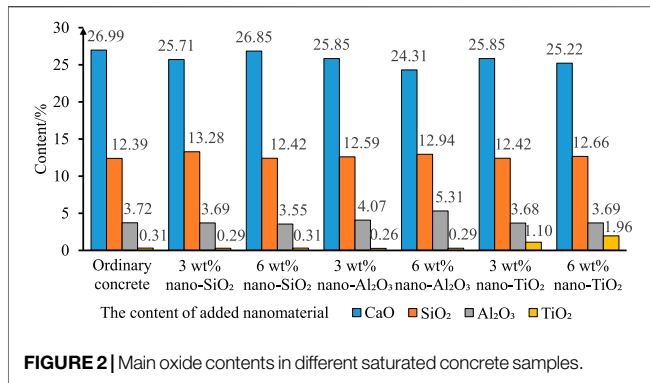
Materials

The materials used in this study included cement, river sand, stones, nano-SiO₂, nano-Al₂O₃, nano-TiO₂, and a water-reducing agent. Portland cement (PO42.5) was used in this experiment, and it was the main cementitious material used for making concrete materials, and its chemical composition

table is shown in **Table 1**. The river sand was taken from the river channels around the city, with yellow color and low mud content. The particle size of the stone was between 5 and 10 mm, with cyan color, high calcium content, and good workability. The particle size of the three nanomaterials is all 30 nm. The purity of the three nanomaterials was 99%. The water-reducing agent uses polycarboxylic acid high-performance water-reducing agent, which can improve the fluidity and strength of concrete.

Mixing Method

Two types of samples were prepared: ordinary saturated concrete samples without nanomaterials for reference and comparison. In subsequent research, this type of sample was called an ordinary saturated concrete sample, the other was the nano-saturated concrete samples, which were used to study the modifying



effects of different types and contents of nanomaterials on the mechanical properties and microstructure of saturated concrete. The ordinary saturated concrete samples were mixes of cement, river sand, and stones in the ratio of 1: 2: 2, with a water-cement ratio of 0.6 and a water-reducing agent content of 0.2% of the cement mass, made without addition of nanomaterials. For nano-saturated concrete materials, two control parameters for the content and type of nanomaterials were designed. The contents of nanomaterials included 3 wt% and 6 wt%. The added nanomaterials replaced the corresponding quantity of cement. There were three types of nanomaterials used here: nano-SiO₂, nano-Al₂O₃, and nano-TiO₂. Through the changes of these two control parameters, there were six different types of nano-saturated concrete samples. In summary, a total of seven types of concrete were prepared in the present research (four samples of each type, and a total of 28 samples were prepared). The mass ratio of raw materials of each type of concrete samples is summarized in **Table 2**.

For nano-concrete materials, a series of steps were needed to prevent the agglomeration of the added nanomaterials. Firstly, nanomaterials of the required quality were put into water and dispersed using an ultrasonic cleaning machine for 15 min to ensure their even dispersal in the water. Then, the cement, stones, and river sand of the quality described in **Table 2** were put into a bucket and mixed for 1 min. Finally, the dispersed liquid with its nanomaterials was poured into the bucket and stirred using a mixer for 10 min. The mixed slurry was poured into a mold, and

after waiting for 24 h the mold was removed, as shown in **Figure 1**. The standard cylindrical samples of $\Phi 50 \times 100$ mm were drilled from the condensed paste after demolding. A total of 28 samples were then drilled: to ensure that the concrete samples reached a state of fully saturation, after drilling they were soaked in sodium hydroxide solution with a pH of 8 for water saturation treatment. After 12 days, the samples were removed for subsequent testing. In this paper, the water retention process of concrete lasts for 12 days, so it is considered that the concrete samples have reached a fully saturated state.

Experimental Equipment

X-Ray Fluorescence (XRF)

The debris produced during sample processing was ground into 200-mesh powder using an agate mortar. Then, the element and oxide content were tested by X-ray fluorescence spectrometer (Arl Perform[®]X).

Scanning Electron Microscopy

The debris produced during sample processing was made into a sample of 1 cm² cross-sectional area. To observe the microstructure and pore state of different types of saturated concrete samples, the Quanta 200 F field emission environment scanning electron microscope produced by FEI was used.

Uniaxial Compression Testing

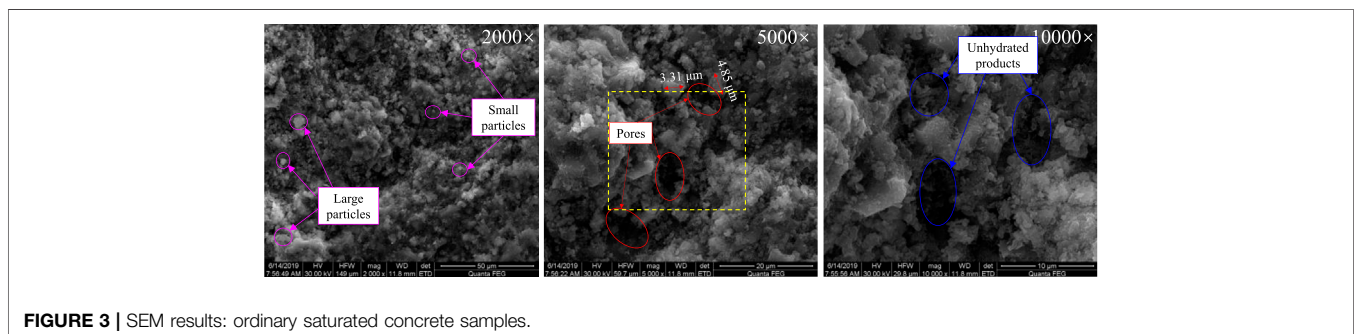
The uniaxial compression testing of saturated concrete samples was performed using an RTR-1000 triaxial rock mechanics test system (GCTS Co., United States).

COMPOSITION AND MICROSTRUCTURE

X-Ray Fluorescence (XRF)

The XRF results show that: the amount of CaO in concrete is the highest, indicating that it is the main oxide present in such concrete samples. Therefore, the CaO content and the content of various kinds of nanomaterials (SiO₂, Al₂O₃, and TiO₂) in various types of concrete samples are plotted to compare the oxide content in different saturated concrete samples (**Figure 2**).

It can be seen from **Figure 2** that the amount of CaO in each sample is around 26%, and there is no obvious difference between



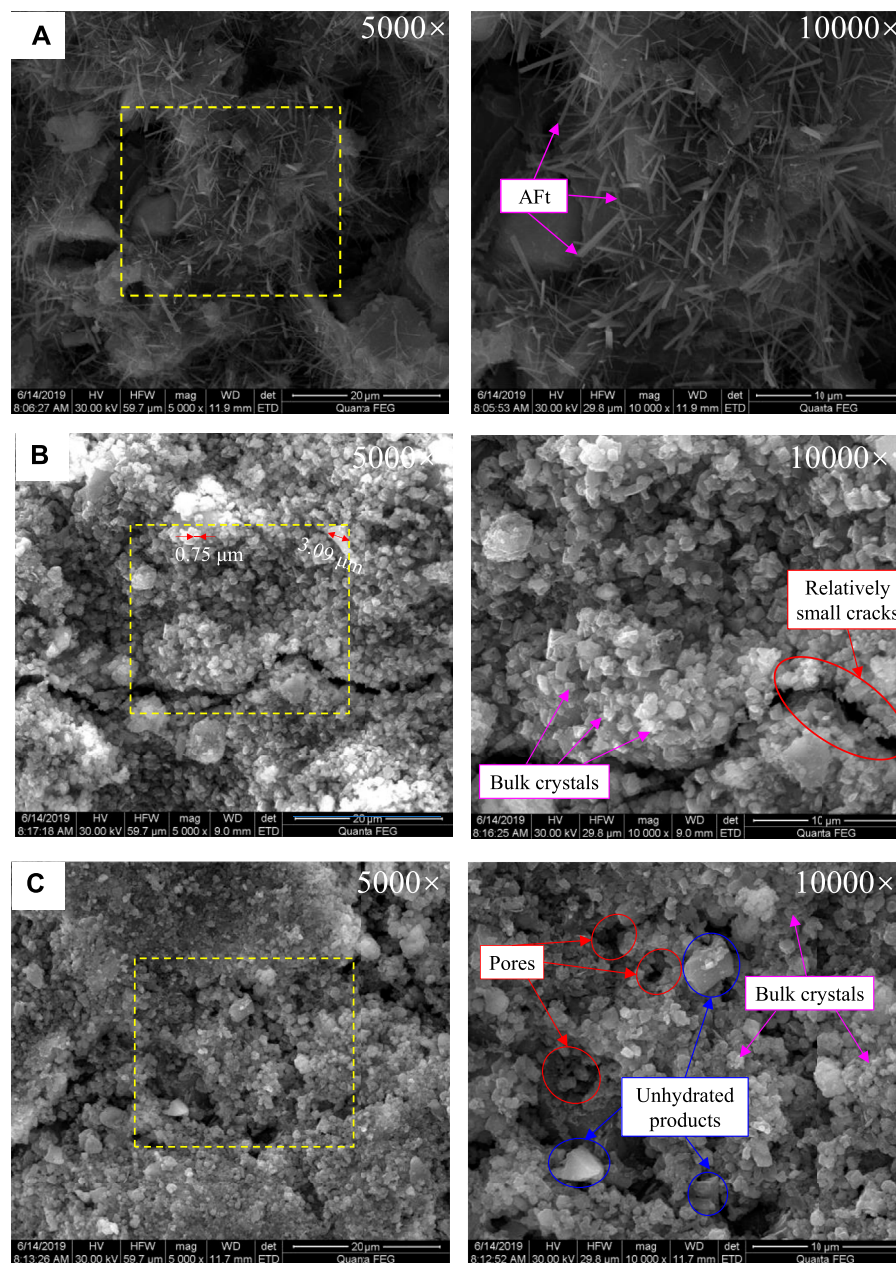


FIGURE 4 | SEM results: saturated concrete containing nanomaterials, **(A)** sample containing nano-SiO₂; **(B)** sample containing nano-Al₂O₃; **(C)** sample containing nano-TiO₂.

them. As one of the main components of concrete materials, SiO₂ accounts for a relatively large proportion of the concrete. Due to the amount of added nano-SiO₂ being relatively small, for samples containing nano-SiO₂, the content of SiO₂ shows no significant change compared with other samples; however, the Al₂O₃ and TiO₂ contents of samples containing nano-Al₂O₃ or nano-TiO₂ increase significantly. The average content of Al₂O₃ in the samples without nano-Al₂O₃ is 3.67%. The average content of Al₂O₃ in the samples mixed with 3 wt% nano-Al₂O₃ is 3.67%. The average content of Al₂O₃ in the samples mixed with 6 wt%

nano-Al₂O₃ is 4.07%. The average content of TiO₂ in the samples without nano-TiO₂ is 0.29%. The average content of TiO₂ in the samples mixed with 3 wt% nano-TiO₂ is 1.1%. These results indicate that the nanomaterial has been successfully mixed with concrete through the mixing method outlined in *Mixing Method*.

Scanning Electron Microscopy

The SEM scanning results of ordinary saturated concrete samples are shown in **Figure 3**: particulate hydration products in ordinary

TABLE 3 | Wave velocities.

	Number	Length (mm)	Time (μ s)	Wave velocity (m/s)	Standard deviation
Ordinary saturated concrete samples	C-1	105.24	37.6	2,798.94	71.03
	C-2	99.94	38	2,630	
	C-3	100.64	38.4	2,620.83	
	C-4	100.53	37.6	2,673.67	
The saturated concrete samples containing 3 wt% nano-SiO ₂	S-1	99.47	38.4	2,590.36	17.96
	S-2	100.31	38.4	2,612.24	
	S-3	100.11	38.4	2,607.03	
	S-4	100.33	38	2,640.26	
The saturated concrete samples containing 6 wt% nano-SiO ₂	S-5	99.42	38.8	2,562.37	21.71
	S-6	100.04	38.8	2,578.35	
	S-7	99.93	39.2	2,549.23	
	S-8	99.76	39.6	2,519.19	
The saturated concrete samples containing 3 wt% nano-Al ₂ O ₃	A-1	100.4	37.6	2,670.21	13.03
	A-2	100.42	37.6	2,670.74	
	A-3	100.37	37.2	2,698.11	
The saturated concrete samples containing 6 wt% nano-Al ₂ O ₃	A-5	100.17	37.1	2,700	77.13
	A-6	100.54	40.1	2,507.23	
	A-7	100.79	37.6	2,680.59	
	A-8	100.68	38.9	2,588.17	
The saturated concrete samples containing 3 wt% nano-TiO ₂	T-1	100.17	37.6	2,664.10	13.81
	T-2	100.13	37.6	2,663.03	
	T-3	99.76	37.2	2,681.72	
	T-4	100.31	37.2	2,696.51	
The saturated concrete samples containing 6 wt% nano-TiO ₂	T-5	100.84	37.4	2,696.26	19.60
	T-6	100.91	38	2,655.53	
	T-7	100.45	38	2,643.42	
	T-8	100.65	37.8	2,662.70	

saturated concrete samples vary in size and there are many micro-pores therein. There is also a significant amount of loose un-hydrated products seen in the pores and the pores are areas of accumulation of Ca(OH)₂ generated during hydration of the cement. All these combine to make the pores become areas of weakness in saturated concrete.

The microstructure of the three types of saturated concrete samples containing different nanomaterials differs: as shown in **Figure 4A**, many acicular crystals are randomly distributed within samples containing nano-SiO₂, which fill the pores and increase the compactness of the material. In the sample containing nano-Al₂O₃, as shown in **Figure 4B**, the internal hydration products are bulk crystalline in form. The internal hydration products are closely connected with the un-hydrated products, and the large cracks in the concrete are filled with these crystals before becoming relatively small cracks. The hydration product of the sample containing nano-TiO₂ (**Figure 4C**) is like that of the sample containing nano-Al₂O₃, and they are both bulk crystals, but the internal structure of the sample containing nano-TiO₂ is looser than the sample containing nano-Al₂O₃. There are still large pores inside the sample containing nano-TiO₂ and the degree of hydration is lower than that of the sample containing nano-Al₂O₃, and some un-hydrated products remain within.

In summary, compared with the saturated samples without nanomaterials, nanomaterials can improve the microstructure of saturated concrete materials. For the saturated sample containing nanomaterials, on the one hand, the internal

hydration product particles have a smaller diameter and the internal structure is more uniform and compact: such as for ordinary saturated concrete, the internal particle diameter is mostly between 3 and 5 μ m, and for saturated concrete containing with nanomaterials, although there are a few crystals with a particle diameter of 3 μ m, the internal crystal diameter is mostly around 1 μ m; on the other hand, the internal pores are much fewer in number, and the pores are filled with hydration products. This is because nanomaterials exhibit high pozzolanic activity that can promote the hydration reaction of cement, and the secondary hydration reaction with Ca(OH)₂ can produce more C-S-H gel. The secondary hydration products are filled in the pores: this can increase the content of C-S-H gel in the weak area of the interface and improve the compactness of the slurry and reform the microstructure. Among all saturated concrete samples, the saturated concrete samples containing nano-Al₂O₃ show the best microstructure in that the internal structure is more uniform and compact, and its integrity is optimal.

RESULTS AND ANALYSIS

Wave Velocity Test

Before the saturated concrete samples were subjected to uniaxial compression, the different types of saturated concrete samples were numbered. The ordinary saturated concrete samples were labeled C (a total of four samples). The saturated concrete

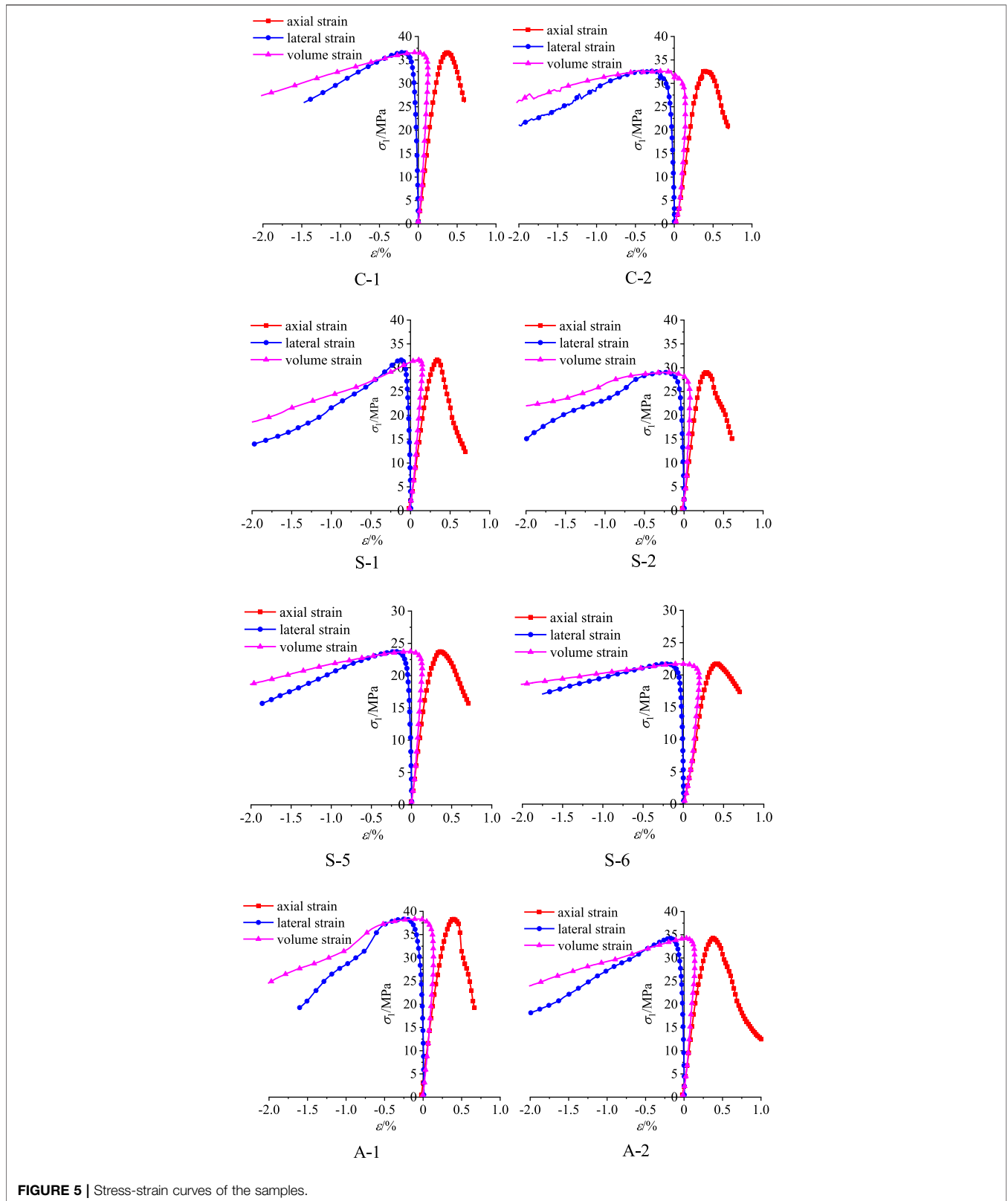


FIGURE 5 | Stress-strain curves of the samples.

samples containing nano-SiO₂ were labeled S (a total of eight samples). The saturated concrete samples containing nano-Al₂O₃ were labeled A (a total of eight samples). The saturated concrete

samples containing nano-TiO₂ were labeled T (a total of eight samples). The wave velocity of each sample was tested with a multi-frequency acoustic wave measurement system. The

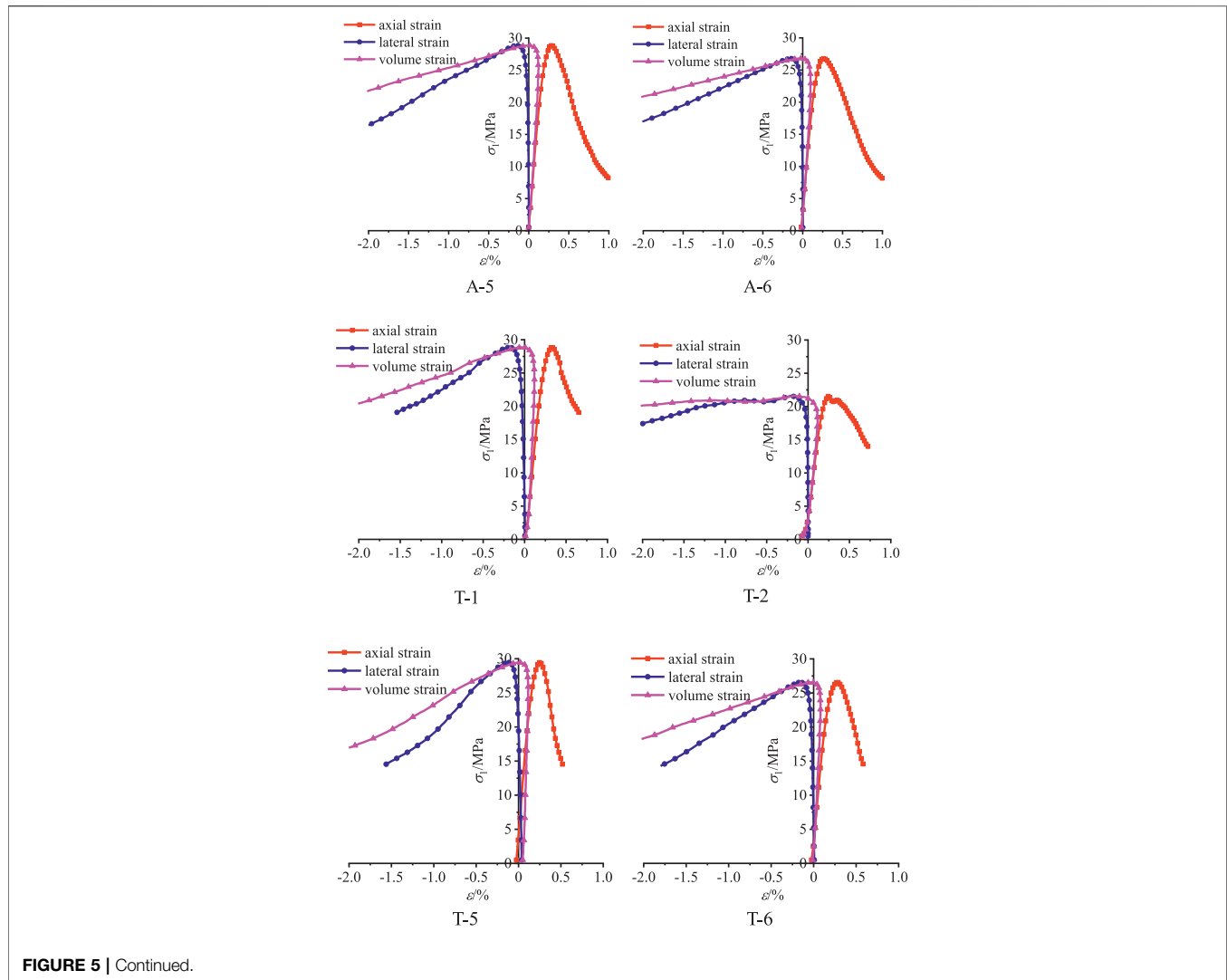


FIGURE 5 | Continued.

numbers of each sample and the results of the wave velocities are shown in Table 3.

Experimental Results: Uniaxial Compression

The axial, lateral, and volumetric stress-strain curves of the samples are shown in Figure 5. Through uniaxial compression experiments, the compressive strength of each sample can be obtained. The elastic modulus, deformation modulus, and Poisson's ratio of these samples can be calculated according to the stress-strain curves.

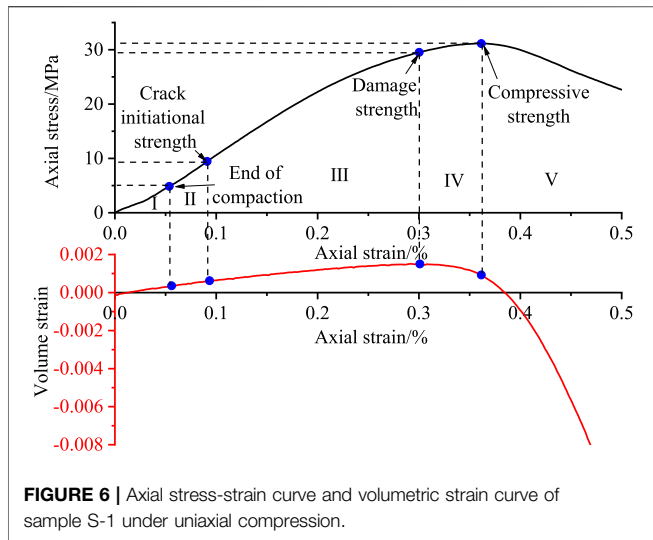
The damage strength is the starting point for unstable crack growth. The damage strength indicates that many cracks are interconnected. It is well known that crack propagation often leads to the failure of concrete (Hao et al., 2016; Gong et al., 2019; Pan et al., 2019; Hao et al., 2020). Therefore, it is necessary to study the damage strength of concrete. The most commonly used method to determine the damage strength is the crack volume strain calculation method (Martin and Chandler, 1994; Cai et al.,

2004). In the present work, the damage strength of the saturated concrete samples is determined according to the crack volume strain calculation method (Eq. 1):

$$\varepsilon_v = \varepsilon_1 + 2\varepsilon_3 \quad (1)$$

where: ε_1 is the axial strain of the saturated concrete sample, ε_2 is the circumferential strain, and ε_v is the volumetric strain.

Sample S-1 is taken as an example to illustrate the characteristics of the stress-strain curve and the method of determination of the damage strength of saturated concrete. The axial stress-strain curve and volumetric strain curve of sample S-1 under uniaxial compression are shown in Figure 6. It can be seen that the axial stress-strain curve and volumetric strain curve of saturated concrete are divided into five stages: crack closure (Stage I), elastic behavior (Stage II), stable crack growth (Stage III), unstable crack growth (Stage IV), and failure (Stage V). In Stage I, the crack volumetric strain is positive, and the slope of the curve is positive, which indicates the initial cracks, pores, etc. inside the sample are closed under axial stress, resulting in reduction in the volume of the crack and the sample.



In the elastic stage (Stage II), the axial stress-strain curve is quasi-linear, and the slope of the curve remains practically unchanged. At this stage, the volume strain of the sample is mainly elastic volume strain, there is almost no crack initiation inside the sample, and the crack volume strain has no obvious change. During stable crack growth (Stage III), the slope of the stress-strain curve begins to decrease. At this stage, cracks begin to occur inside the sample and begin to gradually expand; because the volumetric strain increases upon crack opening, the slope of the volume strain curve in this stage gradually decreases, that is, the rate of change of sample volume decreases. During unstable crack growth (Stage IV), the stress-strain graph becomes non-linear and a peak appears therein. The slope of the stress-strain curve decreases with increasing load, and the rate of change of strain also increases. Many cracks penetrate through the sample, and the volume of the sample begins to increase. Due thereto, the slope of the volumetric strain curve becomes negative. After the stress reaches its peak value, the sample begins to fail (Stage V): the sample volume increases rapidly, and the volumetric strain continuously decreases. Therefore, the demarcation point between the elastic stage and the stable crack growth stage, that is, the stress value corresponding to the inflection point of the crack volume strain slope from positive to negative is the crack initiation strength of the S-1. the demarcation point between the stable crack growth and the unstable crack growth stage, that is, the stress value corresponding to the inflection point of the volume strain slope from positive to negative is the damage strength of S-1, and the damage strength of sample S1 can be determined to be 29.653 MPa.

Using the same method, the damage strength of all samples can be determined. The compressive strength, damage strength, elastic modulus, deformation modulus, and Poisson's ratio of each sample are listed in **Table 4**.

Analysis

According to the measured compressive strength and wave velocity of ordinary saturated concrete samples, the

compressive strength of ordinary saturated concrete samples corresponding to arbitrary wave speeds can be calculated by **Eq. 2**. Comparing the compressive strength of the nano-saturated concrete sample with the compressive strength at the same wave velocity of the ordinary saturated concrete sample, the effect of nanomaterial addition on the compressive strength of saturated concrete can be obtained. The effect of nanomaterials on the deformation modulus, elastic modulus, and damage strength can also be compared by the aforementioned methods, so will not be repeated later.

$$\sigma_n = \sigma_{min} + \frac{\sigma_{max} - \sigma_{min}}{v_{max} - v_{min}} \times v_n \quad (2)$$

where: v_n is the wave velocity. σ_n is the compressive strength at the corresponding wave velocity; σ_{min} and σ_{max} are the minimum and maximum compressive strength of ordinary saturated concrete samples, respectively; v_{min} and v_{max} are the minimum and maximum wave velocity of ordinary saturated concrete samples, respectively.

Compressive Strength

The compressive strength of various types of saturated concrete samples is shown in **Figure 7**. It can be seen that the compressive strength of saturated concrete is affected by the addition of nanomaterials, and the modifying effects of different contents and types of nanomaterials on the compressive strength of concrete also vary.

For the saturated concrete samples containing nano-SiO₂, the compressive strength of saturated concrete samples containing 3 wt% nano-SiO₂ is significantly increased compared with that of ordinary saturated concrete samples, with an average increase of 8.56%; however, when the added amount of nano-SiO₂ is increased to 6 wt%, the compressive strength of nano-saturated concrete sample is decreased relative to that of ordinary saturated concrete samples, indicating that the content of 6 wt% nano-SiO₂ has exceeded its optimum level. The above results indicate that the compressive strength of saturated concrete samples does not always increase with the increase of the nano-SiO₂ content. When the content of nano-SiO₂ exceeds a certain value, the addition of nanomaterials not only fails to increase the strength of saturated concrete but decreases it.

For the saturated concrete samples containing nano-Al₂O₃, the compressive strength of saturated concrete samples containing 3 wt% nano-Al₂O₃ is also increased compared with ordinary saturated concrete samples, with an average increase of 20.27%. The modifying effect is better than that in samples containing the same amount of nano-SiO₂. The compressive strength of the samples containing 6 wt% nano-Al₂O₃ shows two different outcomes compared with that of ordinary saturated concrete samples: some are greater than that of ordinary saturated concrete samples, such as A-6 and A-8, with an average increase of 14.69%. The increase is lower than that found with 3 wt% nano-Al₂O₃ while the strength of the remaining samples (A-5 and A-7) is lower than that of ordinary saturated concrete samples, with an average decrease of 9.19%.

TABLE 4 | Experimental results: uniaxial compression.

	Number	Compressive strength/MPa	Damage strength/MPa	Elastic modulus/GPa	Deformation modulus/GPa
Ordinary saturated concrete samples	C-1	36.59	32.27	14.26	9.51
	C-2	32.80	26.81	12.24	8.44
	C-3	27.92	22.34	10.79	6.46
	C-4	35.52	30.87	14.06	9.50
	Mean value	33.21	28.07	12.84	8.48
Standard value	3.35	3.87	1.42	1.24	
The saturated concrete samples containing 3 wt% nano-SiO ₂	S-1	31.64	29.65	12.49	8.67
	S-2	29.03	23.20	14.14	9.55
	S-3	29.04	19.12	7.80	6.80
	S-4	29.58	21.30	10.22	7.64
	Mean value	29.82	23.32	11.16	8.17
Standard value	1.07	3.93	2.39	1.04	
The saturated concrete samples containing 6 wt% nano-SiO ₂	S-5	23.74	19.12	10.21	6.35
	S-6	21.72	19.12	8.23	5.35
	S-7	20.98	19.84	9.42	6.02
	S-8	22.49	18.69	9.40	6.09
	Mean value	22.23	19.19	9.32	5.95
Standard value	1.02	0.41	0.71	0.37	
The saturated concrete samples containing 3 wt% nano-Al ₂ O ₃	A-1	38.36	29.72	12.69	9.22
	A-2	34.25	29.49	13.18	8.46
	A-3	38.49	32.43	11.66	8.63
	Mean value	37.03	30.54	12.51	8.77
	Standard value	1.97	1.33	0.64	0.33
The saturated concrete samples containing 6 wt% nano-Al ₂ O ₃	A-5	28.87	25.28	15.44	10.03
	A-6	26.81	22.59	15.14	9.31
	A-7	28.68	23.97	15.45	9.64
	A-8	28.87	25.09	14.49	8.21
	Mean value	28.31	24.23	15.13	9.30
Standard value	0.87	1.07	0.39	0.68	
The saturated concrete samples containing 3 wt% nano-TiO ₂	T-1	28.87	23.70	13.80	8.69
	T-2	21.61	17.89	10.65	6.51
	T-3	27.41	22.13	11.81	7.81
	T-4	28.48	23.07	12.84	7.83
	Mean value	26.60	21.70	12.28	7.71
Standard value	2.93	2.27	1.17	0.78	
The saturated concrete samples containing 6 wt% nano-TiO ₂	T-5	29.46	25.92	15.85	10.52
	T-6	26.58	22.72	13.92	8.40
	T-7	27.30	24.91	15.59	10.08
	T-8	26.50	23.95	13.91	8.78
	Mean value	27.46	24.37	14.82	9.45
Standard value	1.19	1.18	0.91	0.88	

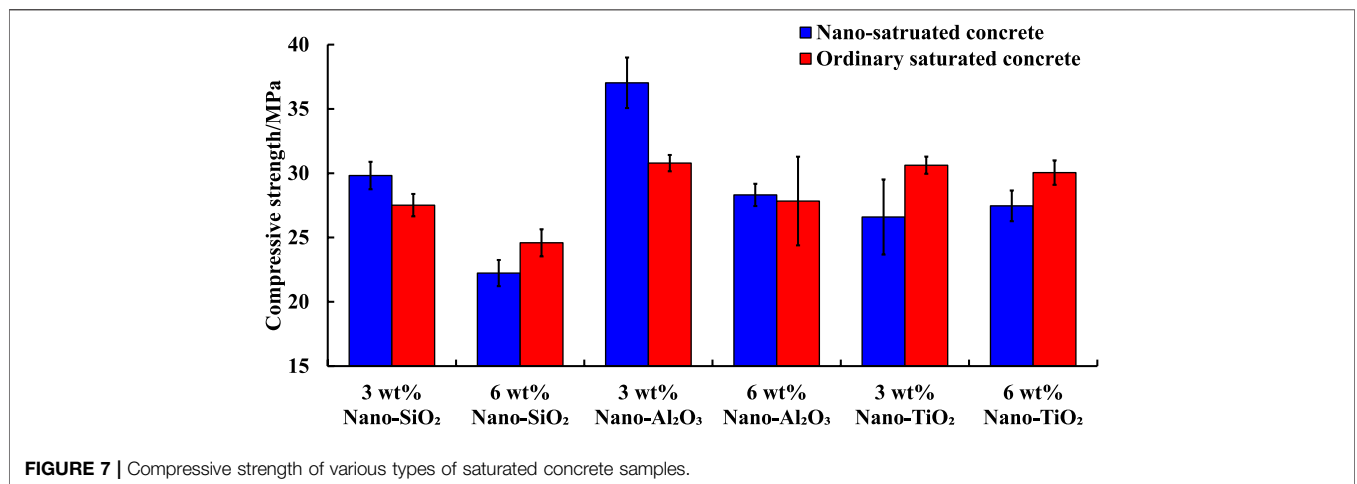


FIGURE 7 | Compressive strength of various types of saturated concrete samples.

indicating that the content of nano- Al_2O_3 has exceeded its optimum content at 6 wt%.

The results of the saturated concrete samples containing nano- TiO_2 are different from the results of nano- SiO_2 and nano- Al_2O_3 . As can be seen from **Figure 7**, the compressive strength of samples containing 3 wt% nano- TiO_2 and 6 wt% nano- TiO_2 is both decreased relative to that of ordinary saturated concrete samples. The reason may be that the nano- TiO_2 has exceeded its optimal content at 3 wt%, which leads to the decrease in compressive strength of saturated concrete samples.

In summary, the compressive strength of saturated concrete can be increased by the addition of nanomaterials, but the compressive strength does not always increase with the increased dosage of nanomaterials. When the amount of added nanomaterial exceeds a certain value, the compressive strength of saturated concrete materials is decreased instead. The optimal content of different types of nanomaterials in concrete samples is also different: when the content of nanomaterials is 3 wt%, the modifying effect of nano- Al_2O_3 on the compressive strength of saturated concrete is the best, followed by that of nano- SiO_2 , whereas with nano- TiO_2 the compressive strength is decreased. At a nanomaterial content of 6 wt%, all nanomaterials have exceeded their optimum content.

In addition, for saturated concrete samples containing nano- SiO_2 and nano- Al_2O_3 , the modifying effect on the compressive strength when the content of nanomaterials is 3 wt% is better than that at 6 wt%, however, the modifying effect of nano- Al_2O_3 on the compressive strength of saturated concrete is better than that of nano- SiO_2 , which is consistent with the modifying effect of nanomaterials on the microstructure seen under the SEM.

Deformation Modulus

The deformation modulus of various types of saturated concrete samples is shown in **Figure 8**: the deformation modulus of saturated concrete samples containing nanomaterials is generally larger than that of ordinary saturated concrete, but the modifying effect of different nanomaterials is different.

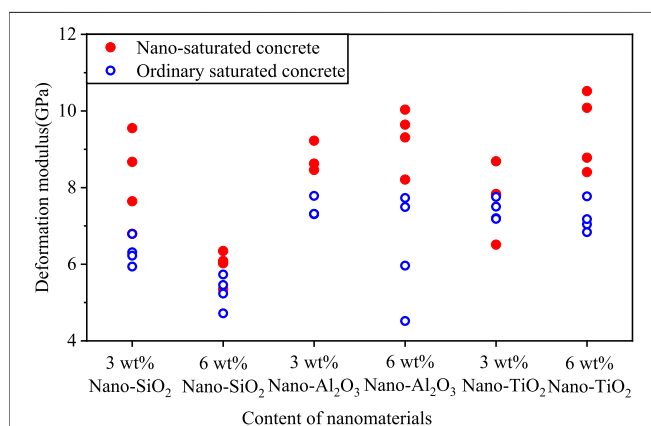


FIGURE 8 | Comparison of deformation modulus of various types of samples.

For saturated concrete samples containing nano- SiO_2 , the deformation modulus of saturated concrete samples containing 3 wt% nano- SiO_2 is increased compared with ordinary saturated concrete samples, with an average increase of 29.77%. The deformation modulus of saturated concrete samples containing 6 wt% nano- SiO_2 is also increased compared with ordinary saturated concrete samples, with an average increase of 13.39%. This shows that the modifying effect on the deformation modulus of saturated concrete when the content of nano- SiO_2 is 3 wt% is better than that at 6 wt%.

For saturated concrete samples containing nano- Al_2O_3 , the deformation modulus of saturated concrete samples containing 3 wt% nano- Al_2O_3 is increased compared with that of ordinary saturated concrete samples, with an average increase of 17.57%. The deformation modulus of saturated concrete samples containing 6 wt% nano- Al_2O_3 is also increased compared with that of ordinary saturated concrete samples, with an average increase of 50.56%. This shows that the modifying effect on the deformation modulus of saturated concrete when the nano- Al_2O_3 content is 6 wt% is better than that at 3 wt%.

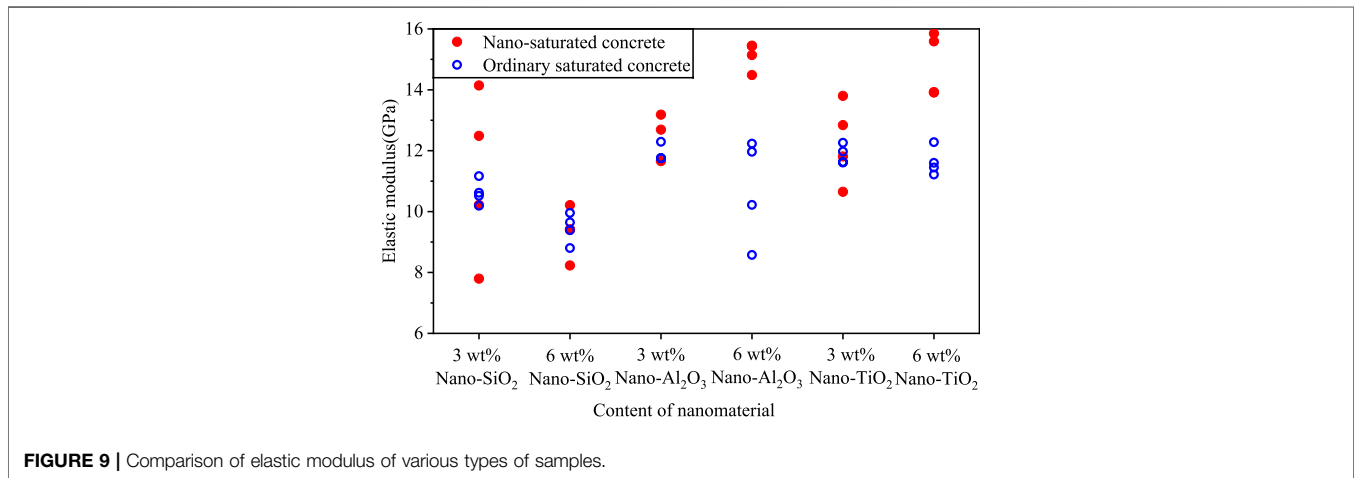
For the saturated concrete samples containing nano- TiO_2 , the deformation modulus of saturated concrete samples containing 3 wt% nano- TiO_2 is increased compared with that of ordinary saturated concrete samples, with an average increase of 4.08%. The deformation modulus of saturated concrete samples containing 6 wt% nano- TiO_2 is also increased compared with that of ordinary saturated concrete samples, with an average increase of 31.11%. This shows that the modifying effect on the deformation modulus of saturated concrete when the nano- TiO_2 content is 6 wt% is better than that at 3 wt%.

These results can be explained by the fact that the addition of nanomaterials to the saturated concrete material can increase the deformation modulus, that is, the stiffness of the saturated concrete is increased. The optimal amount of different nanomaterials in saturated concrete also varies: the modifying effect of 3 wt% nano- SiO_2 on the deformation modulus of saturated concrete is better than that at 6 wt% nano- SiO_2 . For nano- Al_2O_3 and nano- TiO_2 , the modifying effect of 6 wt% nanomaterials on the deformation modulus of saturated concrete is better than that at 3 wt%. Among all the samples tested here, the modifying effect of 6 wt% nano- Al_2O_3 on the deformation modulus of saturated concrete is the best.

It can also be seen from the figure that, although the deformation modulus of most saturated concrete samples containing nanomaterials is greater than that of ordinary saturated concrete samples, there are a few exceptions: for example, the deformation modulus of S-6 and T-2 is lower than that of ordinary saturated concrete samples. The results in **Discussion section** show that the compressive strength of these two samples is also far lower than that of ordinary saturated concrete.

Elastic Modulus

The elastic modulus of various types of saturated concrete is shown in **Figure 9**. The comparison of elastic modulus between the nano-saturated concrete and ordinary saturated concrete is similar to that undertaken for deformation modulus (except for



those samples containing 6 wt% nano-SiO₂, with little significant difference from that of ordinary saturated concrete).

Damage Strength

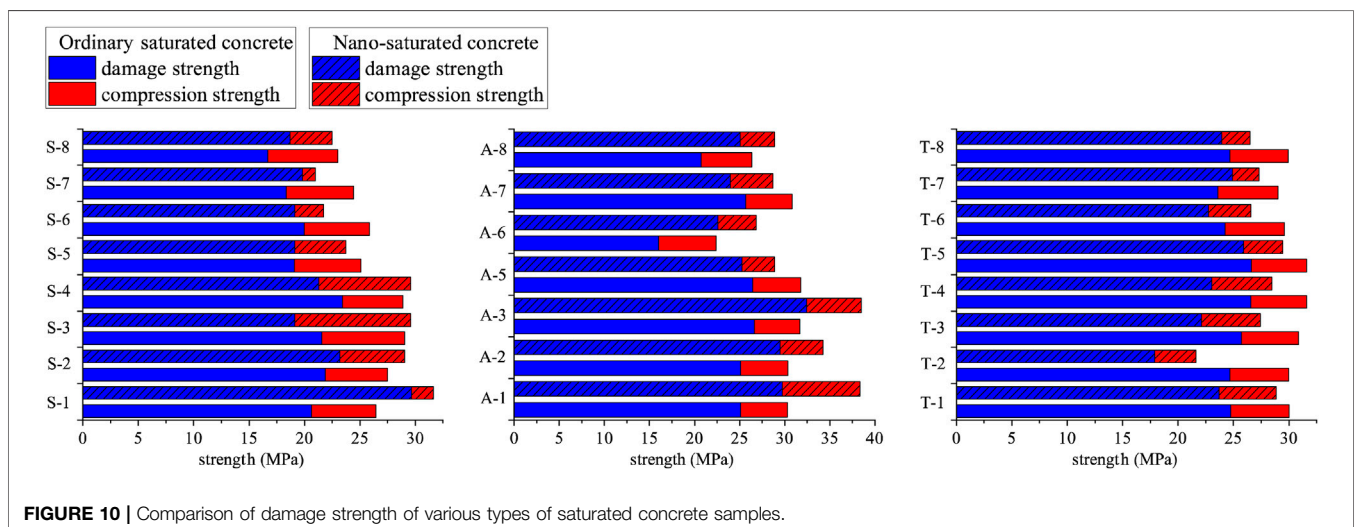
The damage strength of various types of saturated concrete is shown in **Figure 10**: for the saturated concrete sample containing nano-SiO₂, when the content of nano-SiO₂ is 3 wt% (S-1, S-2, S-3, and S-4), the damage strength of S-1 and S-2 is larger than that of ordinary saturated concrete, the damage strength of S-3 and S-4 is less than that of ordinary saturated concrete, but the average damage strength of nano-saturated concrete is larger than that of ordinary saturated concrete. When the content of nano-SiO₂ is 6 wt% (S-5, S-6, S-7, and S-8), the damage strength of S-7 and S-8 is larger than that of ordinary saturated concrete samples, the damage strength of S-6 is less than that of ordinary saturated concrete samples, and the damage strength of S-5 is similar to that of ordinary saturated concrete samples.

For the saturated concrete sample containing nano-Al₂O₃, when the nano-Al₂O₃ content is 3 wt% (A-1, A-2, and A-3), the

damage strength of nano-saturated concrete samples is larger than that of ordinary saturated concrete samples, and the modifying effect of 3 wt% nano-Al₂O₃ on the damage strength of saturated concrete is significantly better than that of the relative content of nano-SiO₂. When the nano-Al₂O₃ content is 6 wt% (A-5, A-6, A-7, and A-8), the damage strength of some samples (A-6 and A-8) is larger than that of ordinary saturated concrete samples, and the damage strength of other samples (A-5 and A-7) is less than that of ordinary saturated concrete samples.

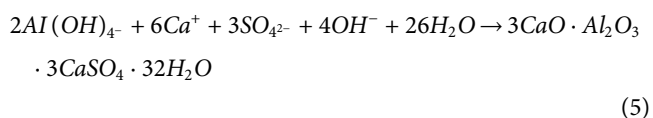
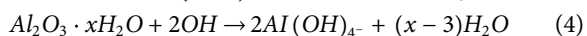
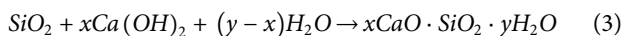
For the saturated concrete sample containing nano-TiO₂, except for T-7, the damage strength of ordinary saturated concrete samples is larger than that of nano-saturated concrete samples.

In summary, for saturated concrete samples containing nano-SiO₂ and those saturated concrete samples containing nano-Al₂O₃, the damage strength of the saturated concrete is increased by the addition of nanomaterials when the content thereof is 3 wt%, and the modifying effect of 3 wt% nano-Al₂O₃ on the damage strength of saturated concrete is significantly



better than that of same relative amount of nano-SiO₂. When the content of nanomaterials is 6 wt%, the addition thereof has a little effect on the damage strength. For the saturated concrete sample containing nano-TiO₂, when the content of nano-TiO₂ is 3 wt%, the content may have exceeded its optimal level in saturated concrete, therefore, the addition of nano-TiO₂ reduces the damage strength of saturated concrete.

Through the above analysis, it can be seen that adding nanomaterials to saturated concrete can optimize its microstructure and improve its strength, modulus and other mechanical properties. The main reasons are the following two aspects: on the one hand, nanomaterials have a small particle size and can fill the internal pores of concrete. On the other hand, nanomaterials have higher specific surface energy, which can promote and participate in the hydration reaction of cement, reacting off excess Ca(OH)₂ (harmful to mechanical properties), and generate more C-S-H gels and other materials, which can improve mechanical properties, as shown in Eqs. 3, 4, 5.



It can also be seen from the formula that both nano SiO₂ and nano Al₂O₃ can participate in the hydration reaction of cement, while nano TiO₂ only can promote the hydration reaction of cement, which leads to the poor mechanical properties of saturated concrete samples containing nano TiO₂ compared with the other two nanomaterials. And the nano-SiO₂ and nano-Al₂O₃ participate in the cement hydration reaction to produce different products, resulting in different microstructures of the two samples. The difference in the microstructure also determines the difference in mechanical properties.

DISCUSSION

The compressive strength of concrete is affected by the amount of nanomaterial added to the concrete, and the extent of this influence may be affected by the properties of the concrete. The saturation of the concrete may also be one of the influencing factors, however, no research has been done on the different effects of nanomaterial contents on the compressive strength of saturated concrete and dry concrete (Rossi et al., 1992; Ross et al., 1996; Yaman et al., 2002a; Yaman et al., 2002b; Wang and Li, 2007; Zheng and Li, 2010; Jin et al., 2012).

To compare the different effects of nanomaterial contents on the compressive strength of saturated concrete and dry concrete, the compressive strength of saturated concrete (in this paper) and dry concrete (Li et al., 2006b; Zhang and Li, 2006; Nazari and Riahi, 2011; Said et al., 2012; Mohseni et al., 2015; Rong et al., 2015; Su et al., 2017; Niewiadomski et al.,

2018; Ren et al., 2018; Du, 2019) when the nanomaterial content was 3 wt% and the nanomaterial content exceeded 3 wt% was analyzed.

The changes in compressive strength of nano-saturated concrete and nano-dry concrete compared to ordinary concrete are shown in **Figure 11** (at a nanomaterial content of 3 wt%). For the concrete samples containing nano-SiO₂ and nano-Al₂O₃, when the nanomaterial content is 3 wt%, although the increase in compressive strength of nano-saturated concrete and nano-dry concrete compared to ordinary concrete is different, the compressive strength of nano-saturated concrete and nano-dry concrete is increased compared to that of ordinary concrete.

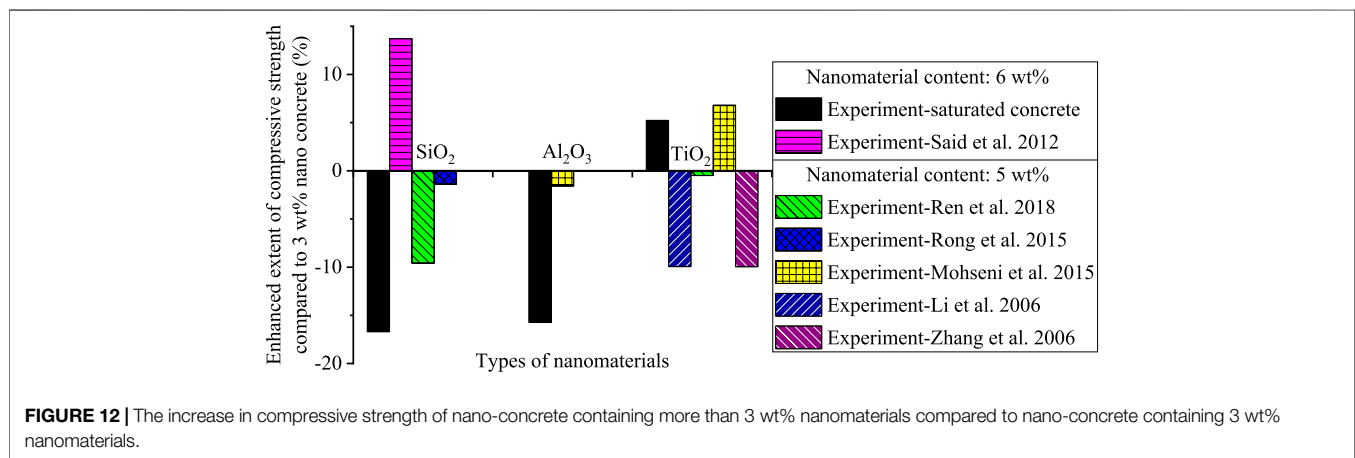
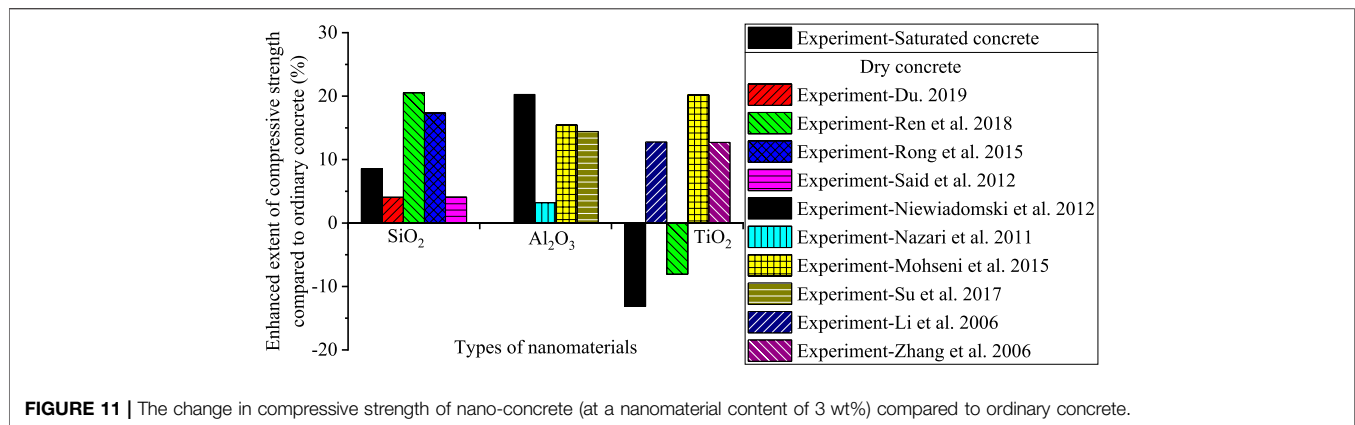
For concrete sample containing nano-TiO₂, when the nano-TiO₂ content is 3 wt%, the compressive strength of nano-saturated concrete is lower than that of ordinary concrete, but the compressive strength of nano-dry concrete varies compared to ordinary concrete; the compressive strength of most nano-dry concrete samples is higher than that of ordinary concrete. It is reported elsewhere (Siddiqui et al., 2016) that the compressive strength of nano-dry concrete containing 3 wt% nano-TiO₂ is lower than that of ordinary concrete, but the reduction is smaller than that for nano-saturated concrete. This suggests that, when the content of nano-TiO₂ is 3 wt%, the increase in compressive strength of saturated concrete compared to ordinary concrete is lower than that for dry concrete.

The increase in compressive strength of nano-concrete containing more than 3 wt% nanomaterials compared to nano-concrete containing 3 wt% nanomaterials is shown in **Figure 12**: for saturated concrete samples containing nano-SiO₂, when the nano-SiO₂ content exceeds 3 wt%, the compressive strength of the nano-saturated concrete sample decreases compared to that at 3 wt%. For dry concrete samples containing nano-SiO₂, when the nano-SiO₂ content exceeds 3 wt%, the compressive strength of a few samples increases compared to that when the nano-SiO₂ content is 3 wt%, and the compressive strength of most samples decreases, but the decrease in the dry concrete is less than that in the saturated concrete.

For concrete samples containing nano-Al₂O₃, when the nano-Al₂O₃ content exceeds 3 wt%, the compressive strength of each concrete sample decreases compared to that at 3 wt%, but the decrease in the saturated concrete is greatest.

For concrete samples containing nano-TiO₂, when the nano-TiO₂ content exceeds 3 wt%, the compressive strength of the nano-saturated concrete samples increases compared with that at 3 wt%. The compressive strength of most nano-dry concrete samples decreases compared with that at 3 wt%.

These results suggest that the compressive strength of both saturated concrete and dry concrete does not always increase with increasing nanomaterial content. When the content of nanomaterials exceeds its optimal level, the increase in compressive strength of the concrete is reduced: for saturated concrete samples containing more than 3 wt% nano-SiO₂ and saturated concrete samples containing more than 3 wt% nano-Al₂O₃, the compressive strength decreases more compared to nano-concrete samples containing 3 wt% nanomaterials for dry concrete samples. This shows that, when the nano-concrete is



saturated, the modifying effect of nanomaterials on the mechanical properties of concrete is diminished.

CONCLUSION

The mechanical properties of saturated concrete are of importance when ensuring the long-term safe and stable operation of hydraulic structures. In this research, scanning electron microscopy, wave velocity, and uniaxial compression were conducted to assess the influence of different nanomaterials added in different amounts on saturated concrete. The conclusions are as follows:

- By the addition of various kinds of nanomaterials to saturated concrete, the microstructure of saturated concrete can be significantly improved, the internal particles are refined, the porosity is reduced, and the compactness and integrity of the slurry are improved. For three different types of nano-saturated concrete samples, the microstructure of samples containing nano- Al_2O_3 is more uniform and compact, and its integrity is optimal.
- Compared with ordinary saturated concrete, the mechanical properties of saturated concrete such as strength,

deformation modulus, and elastic modulus are significantly improved by the addition of 3 wt% nanomaterials; however, the mechanical properties of saturated concrete do not always increase with the increase of the nanomaterial content. When the nanomaterial content is 6 wt%, the compressive strength of the three types of nano-saturated concrete sample decreases compared with that of ordinary saturated concrete samples. Among all saturated concrete samples tested here, the compressive strength of the saturated concrete sample containing 3 wt% nano- Al_2O_3 is the largest, the deformation modulus of the saturated concrete sample containing 6 wt% nano- Al_2O_3 is the largest.

- For concrete samples containing 3 wt% nano- SiO_2 and those containing 3 wt% nano- Al_2O_3 , the compressive strength of nano-dry concrete sample and nano-saturated concrete sample is larger than that of the ordinary concrete sample, and the increase in compressive strength is similar, but when the nano- SiO_2 and nano- Al_2O_3 contents are 6 wt%, the increase in compressive strength compared to ordinary concrete is decreased, and the weakening effect on the compressive strength of saturated concrete is more obvious. For the sample containing 3 wt% nano- TiO_2 , the compressive strength of most of the nano-dry concrete

samples is increased compared with that of ordinary concrete but the compressive strength of the nano-saturated concrete sample is decreased compared with that of ordinary concrete. Compared with dry concrete, when the concrete is saturated, the modifying effect of nanomaterials on the mechanical properties of concrete is diminished.

The artificial dam body of coal mine underground reservoir is complicated in force. In addition to compressive stress, it will also be affected by static forces such as tensile stress and shear stress, as well as dynamic forces such as mining and earthquakes. The mechanical behavior of nanomodified concrete under different stress states will be studied later.

DATA AVAILABILITY STATEMENT

The raw data supporting the conclusion of this article will be made available by the authors, without undue reservation.

REFERENCES

- Bian, H., Jia, Y., Pontiroli, C., and Shao, J.-F. (2017). Numerical Modeling of the Elastoplastic Damage Behavior of Dry and Saturated concrete Targets Subjected to Rigid Projectile Penetration. *Int. J. Numer. Anal. Methods Geomech.* 42 (10), 312–338. doi:10.1002/nag.2744
- Cai, M., Kaiser, P. K., Tasaka, Y., Maejima, T., Morioka, H., and Minami, M. (2004). Generalized Crack Initiation and Crack Damage Stress Thresholds of Brittle Rock Masses Near Underground Excavations. *Int. J. Rock Mech. Mining Sci.* 41 (5), 833–847. doi:10.1016/j.ijrmms.2004.02.001
- Cao, S., Xue, G., Yilmaz, E., Yin, Z., and Yang, F. (2021). Utilizing concrete Pillars as an Environmental Mining Practice in Underground Mines. *J. Clean. Prod.* 278, 123433. doi:10.1016/j.jclepro.2020.123433
- Cao, S., Zheng, D., Yilmaz, E., Yin, Z., Xue, G., and Yang, F. (2020). Strength Development and Microstructure Characteristics of Artificial concrete Pillar Considering Fiber Type and Content Effects. *Construction Building Mater.* 256, 119408. doi:10.1016/j.conbuildmat.2020.119408
- Deng, Z. Y. (2012). Mechanical Properties Research on Concrete Block Doped Nano-TiO₂ under the Conditions of Common Conservation. *Appl. Mech. Mater.* 238, 9–12. doi:10.4028/www.scientific.net/AMM.238.9
- Du, H., Du, S., and Liu, X. (2015). Effect of Nano-Silica on the Mechanical and Transport Properties of Lightweight concrete. *Construction Building Mater.* 82, 114–122. doi:10.1016/j.conbuildmat.2015.02.026
- Du, H. (2019). Properties of Ultra-lightweight Cement Composites with Nano-Silica. *Construction Building Mater.* 199, 696–704. doi:10.1016/j.conbuildmat.2018.11.225
- Gong, F., Yan, J., Luo, S., and Li, X. (2019). Investigation on the Linear Energy Storage and Dissipation Laws of Rock Materials under Uniaxial Compression. *Rock Mech. Rock Eng.* 52, 4237–4255. doi:10.1007/s00603-019-01842-4
- Hao, X.-J., Feng, X.-T., Yang, C.-X., Jiang, Q., and Li, S.-J. (2016). Analysis of EDZ Development of Columnar Jointed Rock Mass in the Baihetan Diversion Tunnel. *Rock Mech. Rock Eng.* 49, 1289–1312. doi:10.1007/s00603-015-0829-4
- Hao, X., Du, W., Zhao, Y., Sun, Z., Zhang, Q., Wang, S., et al. (2020). Dynamic Tensile Behaviour and Crack Propagation of Coal under Coupled Static-Dynamic Loading. *Int. J. Mining Sci. Tech.* 30 (5), 659–668. doi:10.1016/j.ijmst.2020.06.007
- Hong, Z.-j., Zuo, J.-p., Zhang, Z.-s., Liu, C., Liu, L., and Liu, H.-y. (2020). Effects of Nano-clay on the Mechanical and Microstructural Properties of Cement-Based Grouting Material in Sodium Chloride Solution. *Construction Building Mater.* 245, 118420. doi:10.1016/j.conbuildmat.2020.118420

AUTHOR CONTRIBUTIONS

XH designed the experiment and samples; YW and ZC prepared samples; YW, ZC, and HZ performed the experiments under the supervision of XH; XH, YW and YN analyzed the data; and XH, YW and ZC write the paper. All authors read and approved the final manuscript.

FUNDING

This article is supported by the National Natural Science Foundation of China (51804309), Yue Qi Young Scholar Project (2019QN02) and Distinguished Scholar Project (2017JCB02) from China University of Mining and Technology (Beijing), Joint Fund of State Key Laboratory of Coal Resources and Safe Mining- and Beijing Outstanding Young Scientist Program (Grant No SKLCRSM20LH01 and BJJWZYJH01201911413037), National Natural Science Foundation of China (51861145403, 51874312, U1910206).

- Jalal, M., Pouladkhan, A., Harandi, O. F., and Jafari, D. (2015). Comparative Study on Effects of Class F Fly Ash, Nano Silica and Silica Fume on Properties of High Performance Self Compacting concrete. *Construction Building Mater.* 94, 90–104. doi:10.1016/j.conbuildmat.2015.07.001
- Jin, L., Du, X., and Ma, G. (2012). Macroscopic Effective Moduli and Tensile Strength of Saturated concrete. *Cement Concrete Res.* 42 (12), 1590–1600. doi:10.1016/j.cemconres.2012.09.012
- Kaji, T., and Fujiyama, C. (2014). Mechanical Properties of Saturated concrete Depending on the Strain Rate. *Proced. Eng.* 95, 442–453. doi:10.1016/j.proeng.2014.12.204
- Li, H., Zhang, M.-h., and Ou, J.-p. (2006a). Abrasion Resistance of concrete Containing Nano-Particles for Pavement. *Wear* 260 (11–12), 1262–1266. doi:10.1016/j.wear.2005.08.006
- Li, Z., Wang, H., He, S., Lu, Y., and Wang, M. (2006b). Investigations on the Preparation and Mechanical Properties of the Nano-Alumina Reinforced Cement Composite. *Mater. Lett.* 60, 356–359. doi:10.1016/j.matlet.2005.08.061
- Liu, R., Xiao, H., Li, H., Sun, L., Pi, Z., Waqar, G. Q., et al. (2018). Effects of Nano-SiO₂ on the Permeability-Related Properties of Cement-Based Composites with Different Water/cement Ratios. *J. Mater. Sci.* 53 (7), 4974–4986. doi:10.1007/s10853-017-1906-8
- Lu, W., Wang, Q., Jiang, B., Xu, S., Liu, B., Zhang, P., et al. (2019). Comparative Study on Bearing Mechanism and Design Parameters of Confined concrete Arch Joints in Deep Soft Rock Roadway. *Int. J. Coal Sci. Technol.* 6, 493–504. doi:10.1007/s40789-019-00272-5
- Martin, C. D., and Chandler, N. A. (1994). The progressive fracture of Lac du Bonnet granite. *Int. J. Rock Mech. Mining Sci. Geomechanics Abstr.* 31 (6), 643–659. doi:10.1016/0148-9062(94)90005-1
- Mohseni, E., Miyandehi, B. M., Yang, J., and Yazdi, M. A. (2015). Single and Combined Effects of Nano-SiO₂, Nano-Al₂O₃ and Nano-TiO₂ on the Mechanical, Rheological and Durability Properties of Self-Compacting Mortar Containing Fly Ash. *Construction Building Mater.* 84, 331–340. doi:10.1016/j.conbuildmat.2015.03.006
- Nazari, A., and Riahi, S. (2011). Effects of Al₂O₃ Nanoparticles on Properties of Self Compacting concrete with Ground Granulated Blast Furnace Slag (GGBFS) as Binder. *Sci. China Technol. Sci.* 54, 2327–2338. doi:10.1007/s11431-011-4440-y
- Niewiadomski, P., Hoła, J., and Cwirzeń, A. (2018). Study on Properties of Self-Compacting concrete Modified with Nanoparticles. *Arch. Civil Mech. Eng.* 18 (3), 877–886. doi:10.1016/j.acme.2018.01.006
- Pan, W., Wang, X., Liu, Q., Yuan, Y., and Zuo, B. (2019). Non-parallel Double-Crack Propagation in Rock-like Materials under Uniaxial Compression. *Int. J. Coal Sci. Technol.* 6, 372–387. doi:10.1007/s40789-019-0255-4
- Ren, J., Lai, Y., and Gao, J. (2018). Exploring the Influence of SiO₂ and TiO₂ Nanoparticles on the Mechanical Properties of concrete. *Construction Building Mater.* 175, 277–285. doi:10.1016/j.conbuildmat.2018.04.181

- Rong, Z., Sun, W., Xiao, H., and Jiang, G. (2015). Effects of Nano-SiO₂ Particles on the Mechanical and Microstructural Properties of Ultra-high Performance Cementitious Composites. *Cement and Concrete Composites*. 56, 25–31. doi:10.1016/j.cemconcomp.2014.11.001
- Ross, C. A., Jerome, D. M., and Joseph, W. T. (1996). Moisture and Strain Rate Effects on Concrete Strength. *ACI Mater. J.* 93 (3), 293–300. doi:10.14359/9814
- Rossi, P., van Mier, J. G. M., Boulay, C., and Le Maou, F. (1992). The Dynamic Behaviour of concrete: Influence of Free Water. *Mater. Structures*. 25, 509–514. doi:10.1007/BF02472446
- Said, A. M., Zeidan, M. S., Bassuoni, M. T., and Tian, Y. (2012). Properties of concrete Incorporating Nano-Silica. *Construction Building Mater.* 36, 838–844. doi:10.1016/j.conbuildmat.2012.06.044
- Shaikh, F., Chavda, V., Minhaj, N., and Arel, H. S. (2017). Effect of Mixing Methods of Nano Silica on Properties of Recycled Aggregate concrete. *Struct. Concrete*. 19 (6), 387–399. doi:10.1002/suco.201700091
- Siddiqui, M. S., Grasley, Z., and Fowler, D. W. (2016). Internal Water Pressure Development in Saturated concrete cylinder Subjected to Coefficient of thermal Expansion Tests: Poroelastic Model. *Construction Building Mater.* 112, 996–1004. doi:10.1016/j.conbuildmat.2016.02.081
- Su, Y., Wu, C., Li, J., Li, Z.-X., and Li, W. (2017). Development of Novel Ultra-high Performance concrete: From Material to Structure. *Construction Building Mater.* 135, 517–528. doi:10.1016/j.conbuildmat.2016.12.175
- Wang, H., and Li, Q. (2007). Prediction of Elastic Modulus and Poisson's Ratio for Unsaturated concrete. *Int. J. Sol. Structures*. 44 (5), 1370–1379. doi:10.1016/j.ijsolstr.2006.06.028
- Wang, H., Wang, L., Song, Y., and Wang, J. (2016). Influence of Free Water on Dynamic Behavior of Dam concrete under Biaxial Compression. *Construction Building Mater.* 112, 222–231. doi:10.1016/j.conbuildmat.2016.02.090
- Yaman, I. O., Aktan, H. M., and Hearn, N. (2002a). Active and Non-active Porosity in concrete Part II: Evaluation of Existing Models. *Mat. Struct.* 35 (2), 110–116. doi:10.1007/BF02482110
- Yaman, I. O., Hearn, N., and Aktan, H. M. (2002b). Active and Non-active Porosity in concrete Part I: Experimental Evidence. *Mat. Struct.* 35 (2), 102–109. doi:10.1007/BF02482109
- Yang, Z., Gao, Y., Mu, S., Chang, H., Sun, W., and Jiang, J. (2019). Improving the Chloride Binding Capacity of Cement Paste by Adding Nano-Al₂O₃. *Construction Building Mater.* 195, 415–422. doi:10.1016/j.conbuildmat.2018.11.012
- Zhang, M.-h., and Li, H. (2006). The Resistance to Chloride Penetration of concrete Containing Nano-Particles for Pavement. *Proc. Spie-int. Soc. Opt. Eng.* 6175, 1–8. doi:10.1117/12.660882
- Zhang, R., Cheng, X., Hou, P., and Ye, Z. (2015). Influences of Nano-TiO₂ on the Properties of Cement-Based Materials: Hydration and Drying Shrinkage. *Construction Building Mater.* 81, 35–41. doi:10.1016/j.conbuildmat.2015.02.003
- Zheng, D., and Li, X. X. (2010). Prediction of Saturate Concrete Elastic Modulus by Considering Pores and Microcracks. *Amr.* 168-170, 594–598. doi:10.4028/www.scientific.net/AMR.168-170.594
- Zhou, J., Zheng, K., Liu, Z., and He, F. (2019). Chemical Effect of Nano-Alumina on Early-Age Hydration of Portland Cement. *Cement Concrete Res.* 116, 159–167. doi:10.1016/j.cemconres.2018.11.007
- Zuo, J.-p., Hong, Z.-j., Xiong, Z.-q., Wang, C., and Song, H.-q. (2018). Influence of Different W/C on the Performances and Hydration Progress of Dual Liquid High Water Backfilling Material. *Construction Building Mater.* 190, 910–917. doi:10.1016/j.conbuildmat.2018.09.146

Conflict of Interest: YW was employed by Zhengzhou Coal Mining Machinery (Group) Co., Ltd.

The remaining authors declare that the research was conducted in the absence of any commercial or financial relationships that could be construed as a potential conflict of interest.

Copyright © 2021 Hao, Wei, Chen, Zhang, Niu, Chen and Huang. This is an open-access article distributed under the terms of the Creative Commons Attribution License (CC BY). The use, distribution or reproduction in other forums is permitted, provided the original author(s) and the copyright owner(s) are credited and that the original publication in this journal is cited, in accordance with accepted academic practice. No use, distribution or reproduction is permitted which does not comply with these terms.